Travert, Jean-Paul; Taccone, Florent; Bacchi, Vito

Modelling runoff for extreme rainfall events on large catchments using TELEMAC-2D

Modelling runoff for extreme rainfall events on large catchments using TELEMAC-2D

Jean-Paul Travert[1], Florent Taccone[1], Vito Bacchi[1]
jean-paul.travert@edf.fr, Chatou, France
[1]: National Laboratory for Hydraulics and Environment, EDF R&D, Chatou, France

Abstract – **The increase in frequency of intense rainfall events throughout the world brings new challenges that necessitate mitigation measures. Some conceptual hydrological models are already used to estimate discharge at outlet of catchments linked to 2D hydrodynamic model to simulate the downstream floods. However, with the increase of computation capacities, it may be possible to use physically based hydraulic models to simulate runoff directly on large catchments. This paper presents a preliminary application of runoff modelling on large catchments using TELEMAC-2D. The goal is to set up a complete methodology for simulating runoff on large scales. First, a convergence study on catchments of different sizes is done to test the model mesh resolution and has shown that the mesh resolution for these specific applications should be at least 25 m. Second, for catchments larger than 50 0000 km², it is possible to decompose them in sub-catchments and chain the simulations from upstream to downstream to address issues such as simulation time or preparation of data on too large scales. Third, initial investigations have underlined a high sensitivity to the water infiltration parameters particularly towards the end of the simulations when different rainfall events are considered over a long period of time. Even though initial results are encouraging, further investigations are recommended to better characterise infiltration and roughness coefficients at this scale, based on a wider variety of rainfall events and catchments.**

Keywords: floods, runoff, large catchments, SWE, infiltration

I. INTRODUCTION

Extreme floods have become more frequent and severe in the recent years exacerbated by climate change. There are numerous recent examples of major floods such as the July 2021 catastrophic flooding events in Germany [1] and in China [2], or the floods of the streets of Agen in France in September 2021 [3]. These extreme events caused human casualties, high economical costs and damages in sensitive areas. To design appropriate mitigation measures, especially under increasing urbanization and decreasing infiltration rates, numerical models are proactive tools widely used.

Conceptual rainfall-discharge models are often used to evaluate the discharge at the outlets of defined catchments during rainfall events. However, a physically based model, that geographically maps the geometry and the physical properties of a watershed, could be more efficient, because it allows using spatialized water depths and velocities data in the catchment with a better accuracy than the conceptual rainfall-discharge models. Some rainfall-discharge models using the Shallow Water Equations (SWE) in 2D, have already been used successfully for extreme events on rather small catchments up to 100 km² [4][5][6].

These models have been tested on small catchments, but there is still a need to test the capacity and the relevance of numerical models as TELEMAC-2D (www.opentelemac.org) to respond to these issues on larger scales. In this context, the main objective of this work is to explore a numerical strategy to simulate runoff on a large catchment with a good accuracy both for discharges and water depths and evaluate the computation cost, necessary for practical applications.

In this paper, the study area and the available data of the chosen event and catchment are presented. Then, a mesh convergence is carried out to check that the models on larger catchment than the literature remain valid. Finally, based on the mesh convergence, a model built by splitting the larger catchment into sub-catchments is presented along with its calibration for the infiltration and bottom friction laws. The results are compared with hydrometric stations within the catchments.

II. STUDY AREA AND DATA

A. Rain event

During the night of the 8th to the 9th of September 2021, extreme rain precipitations have fallen over the South-West of France. More than 130 mm of precipitations were registered over Agen in only a few hours (an absolute record for its hydrometric station), over 50 mm of rainfall on most of the Garonne catchment and even higher amounts locally during the night, as shown in Figure 1.

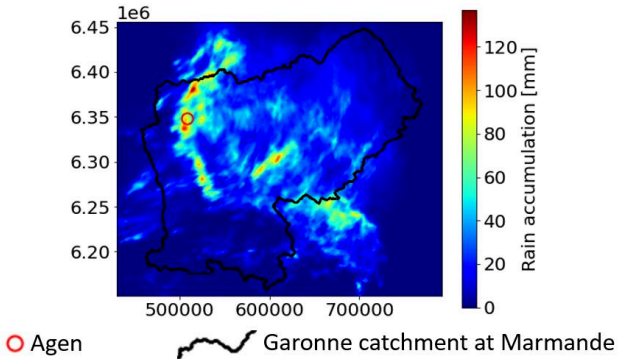

Figure 1. Rain accumulation during the night of the 8th of September.

There were also two other significant events in the following days that will be considered in the model. These rain events happened over the region from the 9th of September at 3

pm to the 10th of September at 5 am and between the 14th of September at 3 pm to the 16th at 2 am.

B. Study area

The study area is the region of Agen and its topographic catchment. Considering that there is no validated data at the hydrometric station of Agen, the outlet of the catchment is placed 50 km downstream of Agen at Marmande where there is a hydrometric station with validated data. The catchment's area can be visualized in Figure 2 (in blue). The area of the catchment (hereafter referred as Garonne catchment) is more than 50 000 km². A smaller sub-catchment (hereafter referred as Hers catchment) is considered, for a purely numerical viewpoint to compare results of the large and small models and to have preliminary results on a smaller scale. This catchment is represented in orange in Figure 2 and is about 786 km².

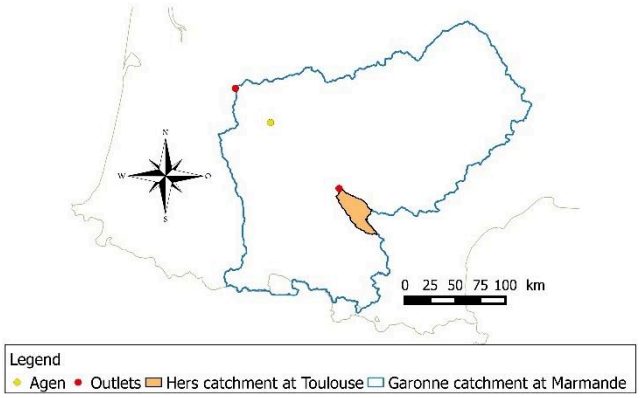

Figure 2. Delineation of the catchments of interest.

C. Data

Most of the data used are open-source data.

Waterways' discharge and water depths are recorded by hydrometric stations that are freely available on a national database (hydro.eaufrance.fr). Within the Garonne catchment, more than thirty hydrometric stations have available data to compare with the results of the model. For instance, in Figure 3 is presented the discharge at the Marmande hydrometric station for the period of 10 days following the start of rainfall. This record is used for the model calibration.

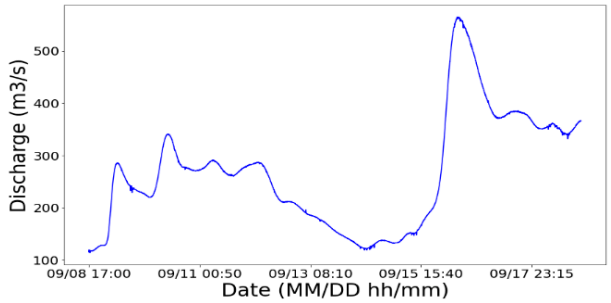

Figure 3. Observed discharge at the hydrometric station of Marmande.

The topography of the numerical model, which is a key parameter when it comes to runoff with SWE, is extracted from the Digital Elevation Map (DEM) of France, at 1 m resolution, measured by Laser Imaging Detection And Ranging (LIDAR), and produced by the National Institute of Geographic and Forest Information (www.ign.fr). The land use is extracted from the Corine Land Cover (CLC) 2018 product provided by the Copernicus Mission, at a resolution of several decametres, and the soil hydrological groups from the Food and Agriculture Organization at a resolution of 250 m. Rainfall data can be extracted from radar products provided by "Météo France", at 1 km resolution every 5 minutes. These data are given in a raster form with the accumulative rainfall over the last 5 minutes for each image. The three events of rain (see section II.A) have been bought from "Météo France". With each image an additional raster is provided to describe the quality of the measurements. On the whole dataset, there are more than 110 000 points of measurements.

III. MATERIAL AND METHOD

The different simulations are performed using the two dimensional (2D) hydrodynamic module (TELEMAC-2D v8p3r1) which solve free-surface flows in the two horizontal dimensions.

A. Overland flow simulation

TELEMAC-2D solves the 2D Shallow Water Equations [7], that are derived from the Navier-Stokes equations, averaged over the vertical with hydrostatic pressure assumption [8].

These equations write, in their conservative form:

$$\begin{cases} \frac{\partial h}{\partial t} + \frac{\partial hu}{\partial x} + \frac{\partial hv}{\partial y} = max(0, R - I) \\ \frac{\partial hu}{\partial t} + \frac{\partial \left(hu^2 + \frac{gh^2}{2}\right)}{\partial x} + \frac{\partial huv}{\partial y} = gh\left(-\frac{\partial z}{\partial x} - S_{fx}\right) \\ \frac{\partial hv}{\partial t} + \frac{\partial huv}{\partial x} + \frac{\partial \left(hv^2 + \frac{gh^2}{2}\right)}{\partial y} = gh\left(-\frac{\partial z}{\partial y} - S_{fy}\right) \end{cases} \quad (1)$$

where h $[m]$ is the water depth, t $[s]$ the time, u $[m \cdot s^{-1}]$ the flow velocity in the x-direction, v $[m \cdot s^{-1}]$ the flow velocity in the y-direction, R $[m \cdot s^{-1}]$ the rain intensity, I $[m \cdot s^{-1}]$ the infiltration rate given by an infiltration model (see section III.D), g $[m \cdot s^{-2}]$ the gravity constant, z [m] the bottom elevation, and S_{fx} $[-]$ and S_{fy} $[-]$ the friction slope in the x- and y-directions.

B. Numerical resolution

An unstructured triangular mesh is used to discretize the domain in space. These type of meshes enable a better adaptation to complex topography of a watershed especially for the river system.

To solve the SWE (1), TELEMAC-2D provides either finite element or finite volume schemes; the work presented here will be based on the finite volume scheme, for which a control volume C_i around each node P_i is constructed as shown in blue in Figure 4. The control volume passes through the centre of gravity for each adjacent node [9].

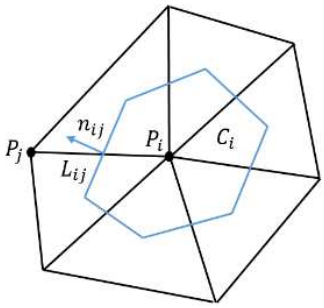

Figure 4. Representation of a control volume for unstructured 2D-meshes.

The SWE (1) are solved with a finite volume scheme. The scheme writes:

$$U_i^{t+1} = U_i^t - \sum_{j \in V_i} \left(\frac{\Delta t}{\Delta x_{ij}} F_{ij}^t + \frac{\Delta t}{\Delta x_{ij}} S_{ij}^t\right), \qquad (2)$$

where $U_i^t = (h_i^t, h_i^t u_i^t, h_i^t v_i^t)$ the state variables at time t at the node P_i, V_i all the nodes surroundings P_i, Δt the time step, $\Delta x_{ij} = \frac{C_i}{L_{ij}}$ with C_i the area of the control volume constructed around the node P_i and L_{ij} the length of the interface between the control volumes C_i and C_j, F_{ij}^t the numerical flux at the interface between C_i and C_j along the normal vector n_{ij} and $S_{ij}^t = \left(R_i - I_i, s_{ijx}^t, s_{ijy}^t\right)$ the source terms of mass and of momentum along x- and y-directions.

The SWE are solved with the equation (2) and the interface fluxes F_{ij}^t are calculated with the Kinetic method [10].

The main difficulty of this method is the representation of the source terms s_{ijx}^t and s_{ijy}^t with regards to the positivity of the water depth, the hydrostatic equilibrium and the management of the dry/wet interfaces for steep slopes. For some combinations of slope, mesh, and water depth, there could be some numerical instabilities generating negative water depths or not preserving the steady state depending on the discretization of these source terms.

To overcome this problem, a hydrostatic reconstruction is used in TELEMAC-2D. The discretization proposed by Chen and Noelle [11] writes:

$$\begin{cases} z_{ij} = min\left(max\left(z_i, z_j\right), min\left(h_i + z_i, h_j + z_j\right)\right) \\ h_{ij} = min\left(h_i + z_i - z_{ij}, h_i\right) \\ S_{ij} = \frac{g}{2}\left(h_i + h_j\right)\left(z_i - z_{ij}\right) n_{ij} L_{ij} \end{cases}, \qquad (3)$$

where S_{ij} represents the slope source term discretization.

C. Friction term

Two friction models have been tested to develop the methodology. At first, the Manning-Strickler law for bottom friction [12] is tested, that writes:

$$V = K_s \cdot R_h^{\frac{2}{3}} \cdot S_f^{\frac{1}{2}}, \qquad (4)$$

where K_s $[m^{\frac{1}{3}} \cdot s^{-1}]$ represents the Strickler coefficient, R_h $[m]$ the hydraulic radius, S_f $[\frac{m}{m}]$ the friction slope and V $[m \cdot s^{-1}]$ the mean velocity of the cross section.

The Strickler coefficients are derived from the characteristics of the catchments using CLC data with land use and related Strickler coefficients from the literature as defined in Table I.

Table I Strickler Coefficients with regards to the land use.

Overall nature of the surface	**Strickler coefficient ($m^{\frac{1}{3}}/s$)**
Waterbodies	35
Fields and meadows without crops	20
Cultivated fields with low vegetation	15 to 20
Cultivated fields with high vegetation	10 to 15
Shrubland and undergrowth areas	8 to 12
Areas of low urbanisation (town)	8 to 10
Highly urbanised areas (agglomeration)	5 to 8

The second model that was used in the catchment application is the friction term defined by Lawrence [13] to spatialize the friction term according to a constant size of roughness k_s $[m]$. This law is physically based and asserts that friction coefficient varies depending on a ratio of inundation $\Lambda = \frac{h}{k_s}$ $[-]$. When the water depth is low compared to the size of the roughness on the soil, the coefficient of friction is then high and inversely as illustrated in Figure 5. When the water accumulates in the hydraulic network the friction is then less important.

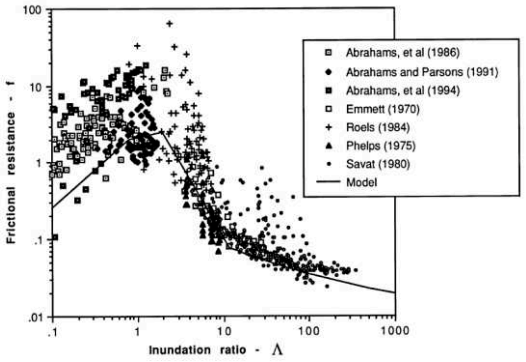

Figure 5. Frictional resistance in function of the inundated ratio [13].

The bottom friction law writes:

$$S_f = \frac{f}{8g} \frac{u|u|}{h}, \qquad (5)$$

with

$$f = \begin{cases} \left(\frac{1}{1{,}64 + 0{,}803\, ln(\Lambda)}\right)^2 & \text{if } \Lambda \geq 10 \\ \frac{10}{\Lambda^2} & \text{else if } 1 \leq \Lambda \leq 10 \\ \frac{8}{\pi} \cdot C_D \cdot min\left(\frac{\pi}{4}, \Lambda\right) & \text{otherwise} \end{cases}, \qquad (6)$$

where S_f $[-]$ is the friction slope, f $[-]$ the Darcy-Weisbach coefficient and C_D $[-]$ the coefficient of drag force of the rough particles fixed to 1 in [13] for roughly spherical particles even if it can vary with the shape of the particles.

It should be noted that this model is not yet included in the TELEMAC-2D official sources and has been added by the authors via specific development.

D. Infiltration model

The model Soil Conservation Service Curve Number (SCS-CN) [14] is a widely used model that is implemented in TELEMAC-2D [15]. This model estimates the net rainfall based on the rough rainfall and a spatially variable coefficient called the Curve Number (CN) that depend on the land use and the soil hydrologic group. For the higher CN, the potential of storage of the soil is lower and there is more runoff. With this model, it is considered that until a certain amount of infiltrated water (called initial abstraction) there is no runoff. Then, a part of the rain is infiltrated, and the other part runs off.

The equations of the model are listed below:

$$\begin{cases} P_e = \frac{(P-Ia)^2}{P+Ia+S} \; if \; P > I_a, \\ Pe = 0 \; otherwise \end{cases} \quad (7)$$

where $P\,[m]$ the rough rainfall, $P_e\,[m]$ the runoff, $S\,[m]$ the potential of storage of the soil and $I_a\,[m]$ the initial abstraction,

with $$S = (\frac{25.4}{CN} - \frac{254}{1000}). \quad (8)$$

The Figure 6 illustrates the principle of this infiltration model.

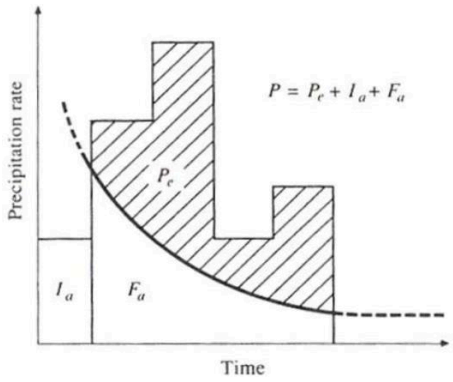

Figure 6. Scheme of principle of SCS-CN [16] .

This 0D model is simple, based on empirical data, and has the advantage of having only one variable CN to calibrate which represents the runoff properties at a node within the unstructured mesh mapping the watershed.

The usual $CN(II)$ values are determined for an initial abstraction of $Ia = 0.2S$ and normal antecedent moisture conditions. For dry ($CN(I)$ lowest runoff potential) or wet ($CN(III$) highest runoff potential) antecedent moistures conditions the CN values can be converted with the following equations [13]:

$$\begin{cases} CN(I) = \frac{4.2 \cdot CN(II)}{10 - 0.058 \cdot CN(II)} \\ CN(III) = \frac{23 \cdot CN(II)}{10 + 0.13 \cdot CN(II)} \end{cases}. \quad (8)$$

And when it is considered $Ia = 0.05S$, then the $CN(II)$ values are changed [17] to:

$$CN(II)_{I_a=0.05S} = \frac{100}{1.879 \cdot \left(\frac{100}{CN(II)} - 1\right)^{1.15} + 1}. \quad (9)$$

It should be noted that in the official sources of TELEMAC-2D numerical model, the routine was not adapted for rain varying in space and has been modified to include this feature.

For the interested reader, the authors also implemented and tested on basic cases the Green-Ampt [18] and Horton [19] models for infiltration with the same design as SCS-CN implementation [15]. These models will be available in the next version of TELEMAC-2D, but they have not been tested on real applications yet, such as the one described in this paper on large catchment.

E. Spatially variable rain

In the real case application, the rain is set spatially in time and space. In the TELEMAC-2D official sources it is already possible to include rain varying in space or in time, but not both simultaneously. In this study, we adapt the wind subroutine to read through a formatted file including the spatially variable rain. It is based on the example "wind_txy" from the official sources of TELEMAC-2D with the wind varying in time and space. In Figure 7 is described the structure of the formatted file for rain spatialization.

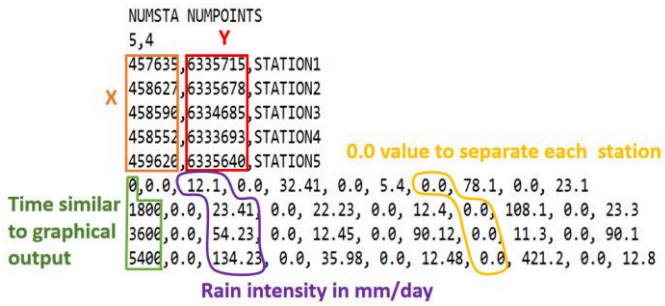

Figure 7. Example of formatted file for varying rainfall in time and space.

The number of stations and measurements should be provided, along with the coordinates of each station. For practical purposes, and to keep the same format as the "wind_txy" example, the time step for graphical output is set the same as for the measurements and the rain intensity is given in mm/day separated by a null value for each station. After reading the formatted file, the interpolation on the mesh is achieved using inverse distance weighting (IDW) method.

IV. MODELS

A two-step approach is presented in this paper. First, a mesh convergence is carried out based on the TELEMAC-2D models covering the whole catchments (Hers and Garonne). Then, the Garonne catchment is split into sub-catchments and results are compared against observations.

Both approaches, described hereafter in sub-section IV.A and IV.B, share similarities. The same numerical schemes described in III.A and III.B are used, and the meshes are both unstructured triangular constructed with BlueKenue (https://nrc.canada.ca). All the simulations are performed on

two of the best High-Performance-Computers (HPC) of EDF R&D.

A. Mesh convergence

1) Geometry

The first goal is to test the sensitivity of the model to the mesh size. A first 100 m resolution mesh was created for the Hers catchment and 800 m for the larger Garonne catchment. Then each triangle was divided by four resulting in resolution divided by two each time. Table II describes the meshes with their respective number of nodes.

Table II Specifications of the different meshes.

Catchment	Resolution [m]	Number of nodes
Hers	100	84 792
Hers	50	337 562
Hers	25	1 347 039
Hers	12.5	5 381 741
Hers	6.25	21 514 137
Garonne	800	84 916
Garonne	400	337 942
Garonne	200	1 348 327
Garonne	100	5 386 429
Garonne	50	21 531 961
Garonne	25	86 100 337

2) Boundary and initial conditions

As for the boundary conditions, a free surface elevation was set up downstream of the domains.

The hydrographic network has not been initialized.

3) Simulation duration

The total simulated time is 111 hours for the smaller catchment and up to 23 days for the larger one to be sure to simulate on larger scales than the time of concentration (time needed for water to flow from the most remote point in a watershed to the watershed outlet).

4) Friction term

For all simulations carried out for the mesh convergence, the Manning-Strickler bottom friction law was used on the Hers and on the Garonne catchments. Figure 8 shows the spatial variation of the Strickler coefficients on the two catchments.

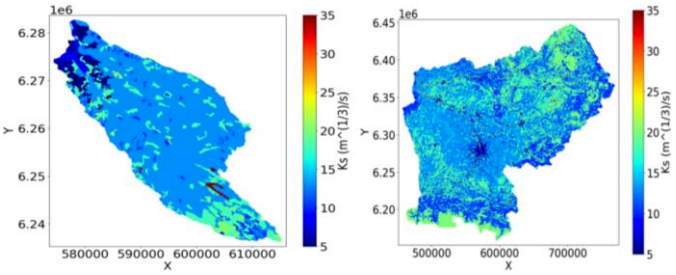

Figure 8. Spatially distributed Strickler friction coefficients (K_S) according to the catchment land-use and land-cover characteristics.

5) Rain inputs

For all simulations carried out for mesh convergence, the input was a constant rain over the domain of one hour with a precipitation rate of 50 mm/h.

B. Sub-catchments splitting application

1) Geometry and splitting of the catchment

The whole catchment is delineated into smaller sub-catchments, as shown in Figure 9.

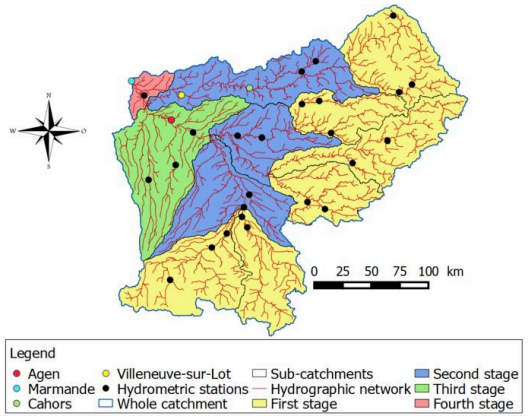

Figure 9. Decomposition of the domain into sub-catchments and hydrometric stations in the catchment.

The Garonne catchment of 50 558 km² has been divided in 11 smaller sub-catchments from 848 km² to 7225 km² from a filled DEM of 100 m resolution by computing the flow directions and the raster of flow accumulation (the functions "r.fill.dir", "r.watershed" and "r.water.outlet" from QGIS 2.6.1 (www.qgis.org) are used). A mesh with a resolution of 25 m (based on the results of the mesh convergence in section V.A) was created on each sub-catchments constrained by the hydrographic network from 1 461 977 to 12 446 175 nodes in their meshes. On each catchment a 25 m resolution DEM is used to extract the elevations and the hydrographic network.

2) Boundary and initial conditions

As for the mesh convergence approach, for each sub-catchment, a free surface elevation was set up downstream. For the catchments in the second to fourth stages in Figure 9, a prescribed discharge is set up upstream, considering the base discharge of the river at the hydrometric stations and the discharge at the outlet of the precedent stages.

The hydrographic network has been initialized in the sub-catchments by retrieving the base discharge before the rainfall event for filling the main river in the catchment, and then the computation restarts from this initial state. An important comment is that the bathymetric data are missing (for rivers the DEM represents the water surface and not the riverbed), and it could have a significant impact in terms of river flow.

3) Chaining of the simulations

The simulations are launched on HPC in parallel from the upstream of the catchment to the downstream by retrieving the discharge at the outlet of the upstream sub-catchments and using the discharge as boundary condition at the inlet of the downstream sub-catchments (as described in section IV.B.2).

The computational process is fully automated from upstream, to downstream with python scripts to create the discharge varying files (for the upstream boundary condition) and linux-bash scripts to chain the TELEMAC-2D simulations and python scripts.

4) Simulation duration

The simulation duration is 10 days on each sub-catchments which is larger than the concentration time of the whole Garonne catchment.

5) Friction term

The chosen bottom friction law is Lawrence. The Manning-Strickler seemed inadequate during initial testing as the CLC is not suited to determine the Strickler parameter within the rivers channel. The CLC map is designed for the flood plains where the roughness coefficients are not calibrated. For instance, in Figure 10, it is shown that along the black line representing the hydrographic network the Strickler coefficient is often too low with this approach.

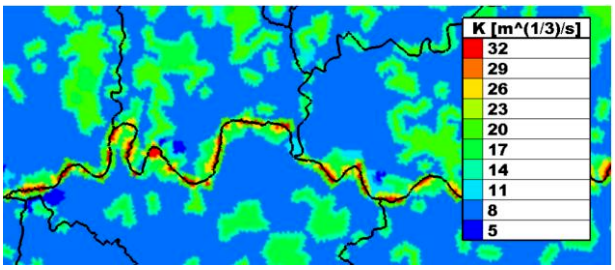

Figure 10. Strickler coefficients within one of the sub-catchments.

Furthermore, the Manning-Strickler law is well-defined for uniform and gradually varying flow but not for runoff with shallow water depths.

6) Rain inputs

The rain is set variable in time and space as explained in section III.E and extracted from the "Météo France" radar data. Only the three events described in section II.A are considered. During the periods between these events, the rainfall is not significant, and the results should not be affected by the lack of data. Indeed, the low rainfall rates between the events would get mostly infiltrated. For the formatted files, extracting all the stations on the whole watershed is not very efficient, and it can be gained three to four hours of simulation by sub-catchment by pre-treating the data and by considering only the stations within each sub-catchment.

V. RESULTS

A. Mesh convergence

In Figure 11 is presented the convergence study with the resolution of the mesh varying between 100 m and 25 m and representing the discharge at the outlet of the Hers catchment for a constant uniform rain of 50 mm/h.

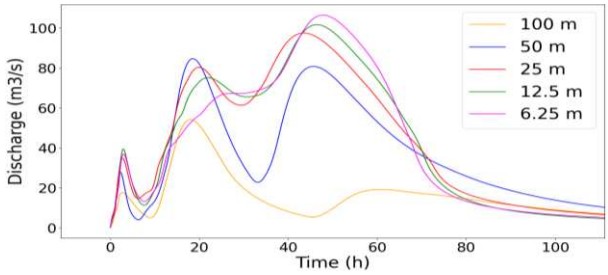

Figure 11. Mesh convergence: discharge at the outlet of Hers catchment.

It appears that the difference of discharge at the outlet between the different meshes is getting closer and is acceptable for a mesh resolution of 25 m. In Table III, the CPU times and the duration of the simulations are given.

Table III Simulation time for the hers catchment.

Resolution [m]	Number of processors	User time [h]	CPU time [days]	Simulated time [h]
100	96	0.03	0.1	111.1
50	96	0.27	1.1	111.1
25	96	3.00	12.0	111.1
12.5	288	8.76	105.1	111.1
6.25	1 056	31.95	1 405.8	111.1

For the 25 m resolution, the simulation time is also reasonable compared to the smaller resolutions, so it appears to be a good compromise between precision and simulation time.

In parallel, some other tests have been carried out to improve the convergence and to try to limit the computational cost. Figure 12 shows a comparison between methods of interpolation of the DEM on the mesh.

It has been tested for the nearest neighbour method (NNM) as well as for the IDW method.

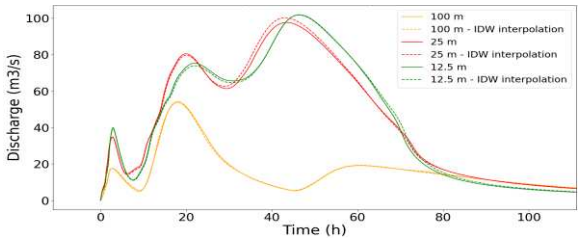

Figure 12. Mesh convergence: difference between NNM and IDW for topography interpolation.

The duration of simulation for both cases is similar, it only changes the time of pre-treatment to create the mesh with IDW that is several hours longer. Using IDW method does not change drastically the results for the discharge at the outlet. Then, it will be chosen to keep with the NNM for the rest of the paper and demonstration.

Another interesting test was to constrain the mesh by forcing the nodes to be placed along the hydrographic network which can be extracted from the DEM. It enables the water to follow the low elevation points and the flows converge in the river network. In Figure 13 are presented the difference

between simulations on different resolution meshes with or without constraint lines.

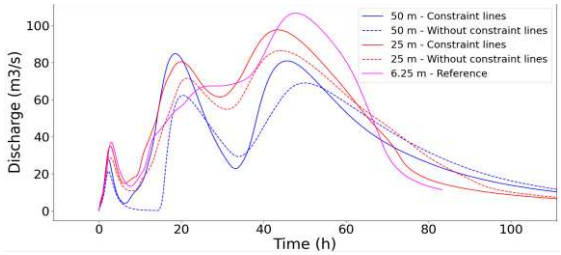

Figure 13. Mesh convergence: discharge at the outlet with and without constraint lines in the meshes.

With constraint lines, the results are closer to the 6.25 m resolution mesh, which is considered as a reference. The simulation time is around 25% longer, as some of the meshed triangles are smaller with the constraint lines, and thus the time step is smaller to preserve the desired Courant number (0.9). It is considered that the difference is worth waiting for a longer simulation because the gain in precision is important.

All these recommendations and first conclusions have been used for the simulations on the larger catchment of the Garonne River at Marmande. The same methodology is used with the same numerical schemes and parameters. In Figure 14 is represented the discharge at the outlet of the catchment for resolution from 800 m to 25 m for a constant rain of 50 mm/h.

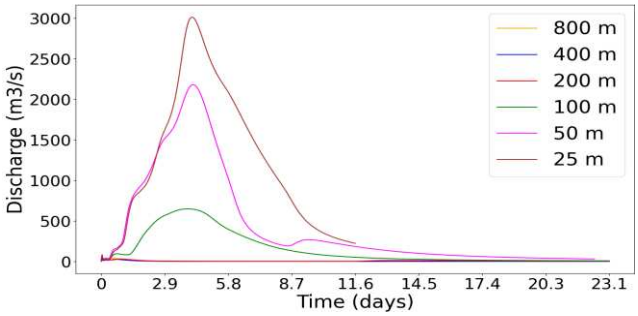

Figure 14. Mesh convergence: discharge at the outlet of Garonne catchment.

These resolutions were used to have similar number of nodes in the mesh as for Hers catchment. For a 25 m resolution mesh the numerical limits are reached, and it is not reasonable to push the convergence further on the large catchment. In Figure 14 there is no convergence before 25 m. Thus, it appears that the use of 25 m resolution mesh (at least) is required for the larger catchment to model the appropriate discharge at the outlet. It could be suggested that if the discharge is sufficiently captured for a resolution of 25 m on the Hers catchment, it can be so for the Garonne catchment, given that both have similar physical and geographical properties and typologies. In Table IV, the simulation times and the CPU times are given.

Table IV Simulation time for the Garonne catchment.

Resolution [m]	Number of processors	User time [h]	CPU time [days]	Simulated time [days]
800	96	/	/	23.1
400	96	/	/	23.1
200	768	0.36	11.7	23.1
100	1152	2.96	142.0	23.1
50	1152	40	1920	23.1
25	2880	55.63	5 575.9	11.6

The user and CPU time is very consequent to achieve the simulation on such a large scale to simulate more than 10 days of physical time even by trying to optimize the use of processors with 20 000 mesh nodes by processor.

The following points can be noted:

- A mesh with a resolution of 25 m is required (at least) to obtain the correct order of magnitude of the discharge at the outlet for the chosen catchments. A finer mesh is too computationally demanding.
- Directly simulating runoff over a catchment of 50 558 km² has proven to be difficult for the chosen catchments because of the long simulation time.
- It is important to extract the hydrographic network with sufficient accuracy and use it to constrain the mesh.

To overcome these challenging points, splitting the whole catchment into smaller sub-catchments is recommended in any case.

B. Sub-catchments splitting application

This approach allows extracting the data and the hydrographic network more easily while using less processors simultaneously. More importantly it becomes less computational costly and more efficient to calibrate the sub-catchments with the hydrometric stations within the catchments. The different hydrometric stations are represented by filled points in Figure 9.

At the time of the redaction of this article, the calibration of the model was not finalized, but preliminary results can already be extracted. The main calibration parameters are the size of the roughness of the soil k_s and the CN for the infiltration model. The CN has been spatialized over the domain as described in section III.D, as can be seen in Figure 15.

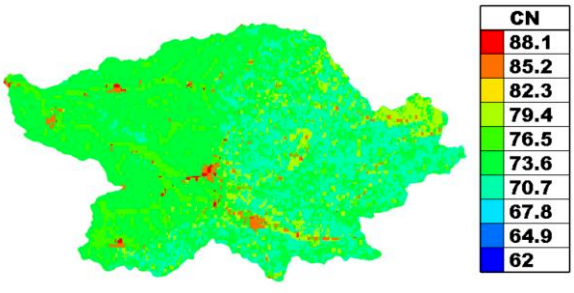

Figure 15. Example of spatialization of CN over one sub-catchment.

For the calibration of the CN parameter, it is proceeded mainly by playing with the antecedent moisture conditions and the initial abstraction ratios ($Ia = 0.2S$ or $Ia = 0.05S$) that are available in the sources of TELEMAC-2D. Some tests of CN sensitivity include variations of the CN values on the whole domain uniformly.

Previous results suggest that the first events of rain are difficult to represent with too much infiltration whatever the chosen parameters of CN or k_s. For the last rainfall event, the runoff following this event is too important on every simulation compared with observed values at the hydrometric stations (Figure 16), because the infiltration rate is getting smaller after the first events of rainfall. In Figure 16, this phenomena at Marmande and at Villeneuve-sur-Lot (Figure 9) within the watershed can be observed.

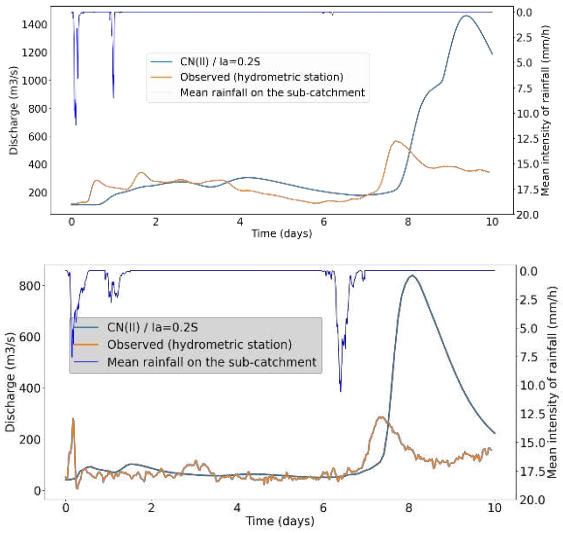

Figure 16. Examples of simulations results for the discharge at Marmande (top) and Villeneuve-sur-Lot (bottom).

Results at Marmande are chosen here because located at the outlet of the entire catchment. At Villeneuve-sur-Lot and Cahors (plotted in Figure 17), they are within an intermediate sub-catchment, therefore showing the dynamic within the global catchment at different places.

For using the SCS-CN model with different events of rain in the simulation, since there was no rainfall for four days between the second and the third event, the water infiltrated stored should decrease. The cumulated storage of infiltration could be partially decreased or totally erased, so the infiltration rate can become higher when there is no rainfall during a certain amount of time before a new rainfall event.

In Figure 17, the discharge is compared with different trials of calibration representing the discharge at Villeneuve-Sur-Lot and Cahors where there are hydrometric stations (Figure 9) in one of the sub-catchments.

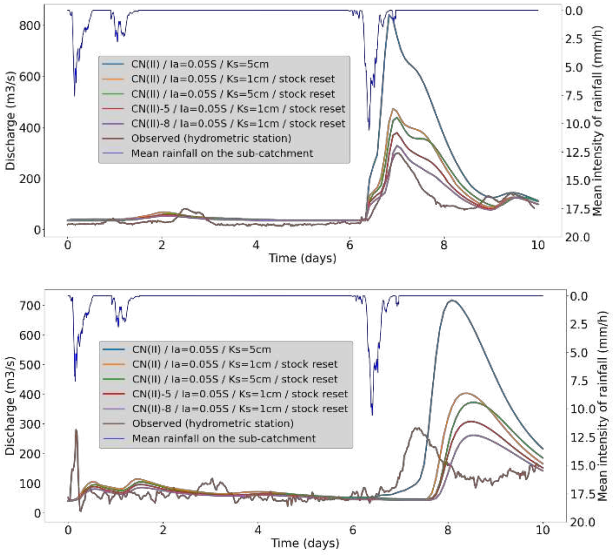

Figure 17. Discharge at Cahors (top) and Villeneuve-sur-Lot (bottom) with different infiltration configurations.

It can be seen, that in a first approach, by taking in a rough way the SCS-CN model the discharge for the second peak is too high (blue plots in Figure 17). So, it has been considered to reset the storage of infiltration in the soil with a null value after the second event of rainfall. And by adjusting the CN and k_s values the good order of magnitude for the discharge can be grasped for the second peak. Depending on the hydrometric stations there are still an important time deviation that must be investigated, with probably some changes needed in the bottom friction law.

The river network is not well represented, because there are no bathymetric data and associated roughness. It is one of the problems that probably explains the time lag that can be observed for some stations. Add a notion of humidity index to use SCS-CN model for following rainfall events as explored in [20] could be promising while playing with the different options and probably adjusting the CN spatialized values as it has been done in the simulation for the red and purple plots by subtracting 5 or 8 to every CN value on the whole domain. The sensitivity to the CN value is a key factor in the calibration that can make it difficult to achieve.

VI. CONCLUSION AND PERSPECTIVES

This paper has presented an introduction and some guidelines to modelling runoff on a large catchment. From the mesh convergence and sub-catchments splitting some key results could be underlined.

First, the mesh convergence has shown that the mesh resolution should be at least 25 m for the chosen catchments to obtain the correct order of magnitude for the discharge at the outlet of the catchment.

For a mesh resolution of that size, the simulation time for large catchment application is very high (on thousands of processors), and it could be complicated to calibrate the model.

It has also been underlined that at this resolution of 25 m with the available DEM data, choosing NNM gives similar

results as IDW method for the interpolation of the elevations on the mesh. For practical purposes the NNM method is recommended.

Using the hydrographic network to constrain the mesh is also recommended. Indeed, the simulation time might be a little longer, but the discharge at the outlet is significantly closer to the reference discharge. However, directly extracting the hydrographic network on catchments of 50 000 km² can be difficult with Geographic Information System software.

The CLC map is adapted for flood plains but not for the channel of rivers. In addition, the Manning-Strickler law may not be suitable for shallow water depths in the case of rainfall. So, the model of friction of Lawrence which is physically based seems more adequate to use with the size of the roughness of the soil that needs calibration.

In view of these challenges, the second approach presented in this paper seems more suited for runoff modelling on large catchments. Indeed, splitting the whole catchment in sub-catchments and chaining the simulations enable the user to prepare the necessary data for the construction of the model more easily. And more importantly, the calibration is easier with the possibility to calibrate each sub-catchments with its own parameters with less computation time and needed processors.

The first results of the calibration with this second approach, have shown that there is a high sensitivity to the calibration parameters (CN and k_s). In addition, the correct order of magnitude on the discharge comparing with observed data cannot be grasped with a naive application of the SCS-CN model. When they are several consecutive rainfall events, the infiltration rate only decreases and cannot go up again. The SCS-CN model is more adapted for a single event of rain. However, it has been presented, that more closer results could be found by decreasing the infiltrated storage in the SCS-CN formula, when there is no significant rainfall for a long period.

Looking ahead, the calibration of the model is not complete, and some modifications in the SCS-CN model of infiltration should be explored, such as considering the humidity index of the soil which can decrease after a certain amount of time without abundant rainfall. Besides, the SCS-CN method may not be the best fit to model runoff on large catchments: new implemented model for infiltration (Horton and Green-Ampt) should be tested as they could be more adapted to the situation. Having said that, the approach could be applied to other large catchments and other rainfall events to validate or not the chosen models. A significant improvement factor is the bathymetry of the rivers (at least the main ones) which is not considered. More data on the bathymetry are needed or it could be explored bathymetric reconstruction with the discharges and the topography.

ACKNOWLEDGEMENT

This research was supported by EDF R&D through the funding of a 6-month internship on the hydraulic modelling of extreme events on large catchments.

REFERENCES

[1] F. Kreienkam, SY. Philip, JS. Tradowsky, SF. Kew, P. Lorenz, J. Arrighi et al., “Rapid attribution of heavy rainfall events leading to the severe flooding in Western Europe during July 2021”, World Weather Attribution, 2021

[2] J. Sun, S. Fu, H. Wang, Y. Zhang, Y. Chen, Y. Wang, H. Tuang, and R. Ma, “Primary characteristics of the extreme heavy rainfall event over Henan in July 2021”, Atmospheric Science Letters, 2022

[3] Météo-Paris, “Bilan des orages et inondations du 8 septembre 2021 dans le sud-ouest, notamment à Agen“, https://www.meteo-paris.com/actualites/bilan-des-orages-inondations-du-8-septembre-2021-dans-le-sud-ouest-notamment-a-agen

[4] F. Taccone, A. Germain, O. Delestre, and N. Goutal, “A new criterion for the evaluation of the velocity field for rainfall-runoff modelling using a shallow-water model”, Advances in Water Resources, 2020, vol. 140, article 103581

[5] P. Brigode, F. Bourgin, R. Yassine, O. Delestre, and P. Lagrée, “Are hydrologic-hydraulic coupling approaches able to reproduce Alex flash-flood dynamics and impacts on southeastern French headwaters?”, SimHydro2021, 2021

[6] R. Yassine, M. Lastes, A. Argence, A. Gandouin, C. Imperatrice, P. Michel, R. Zhang, P. Brigode, O. Delestre, and F. Taccone “Simulation of the Alex storm flash-flood in the Vésubie catchment (south eastern France) using TELEMAC-2D Hydraulic Code”, SymHydro 2021, 2021

[7] A. B. de Saint Venant, « Théorie du mouvement non permanent des eaux, avec application aux crues des rivières et à l’introduction des marées dans leur lit », Rapport technique, Académie des sciences, 1871

[8] J. F. Gerbeau, and B. Perthame, « Derivation of viscous saint venant system for laminar shallow water; numerical validation”, Discrete and Continuous Dynamical Systems, 2001, vol. 1, pp. 89-102

[9] E. Audusse, and M. O. Bristeau, « A well-balanced positivity « second order » scheme for shallow water flows on unstructured meshes”, Journal of Computanional Physics, 2005, vol. 206, no 1, pp. 311-333

[10] E. Audusse, M. O. Bristeau, and B. Perthame, « Kinetic schemes for saint-venant equations with source terms on unstructured grids”, Thèse de doctorat, INRIA, 2000

[11] G. Chen, and S. Noelle, “A new hydrostatic reconstruction scheme based on subcell reconstructions”, SIAM Journal on Numerical Analysis, 2017, vol. 55(2), pp. 758-784

[12] R. Manning, “On the flow of water in open channels and pipes”, Transactions of the Institution of Civil Engineers or Ireland, 1891, vol. 20, pp. 161-207

[13] D.S.L Lawrence “Macroscale roughness and frictional resistance in overland flow”, Earth Surface Processes and Landforms, 1997, vol.22, no 4, pp. 365-382

[14] V. Mockus, National Engineering Handbook, chapter Estimation of Direct Runoff from Storm Rainfall, United States Department of Agriculture, 1972

[15] P.L Ligier, “Implementation of a rainfall-unoff model in TELEMAC-2D”, Proceedings of the XXIIIrd TELEMAC-MASCARET User Conference 2016, 2016, pp. 13-19

[16] U.S. Department of Agriculture, National Resources Conservation Service, National Engineering Handbook, Part 630 Hydrology, Chapter 9 Hydrologic soil-cover complexes, 2004

[17] M. Huang, J. Gallichand, Z. Wang, and M. Goulet, “A modification of the Soil Conservation Service curve number method for steep slopes in the Loess Plateau of China”, Hydrological,2006, vol. 20, pp. 579-589

[18] W. H. Green, and G. A. Ampt, “Studies on soil physics”, The Journal of Agricultural Science, 1911, vol. 4, pp. 1-17

[19] R. E. Horton, “The role of infiltration in the hydrological cycle”, American Geophysical Union, 1933, pp. 446-460

[20] C. Delcourt, F. Taccone, and O. Delestre, “Determination of initial soil moisture for a small highly erodible mountain basin with TELEMAC”, Proceedings of the papers submitted to the TELEMAC-MASCARET User Conference 2021, 2021, pp. 116-122